Air–sea fluxes based on observed annual cycle surface climatology and ocean model internal dynamics: a non-damping zero-phase-lag approach applied to the Mediterranean Sea

David E. Dietrich[a], Robert L. Haney[b], Vicente Fernández[a,*],
Simon A. Josey[c], Joaquín Tintoré[a]

[a] IMEDEA (CSIC-UIB), E-07190 Esporles, Spain
[b] Department of Meteorology, Naval Postgraduate School, Monterey, CA, USA
[c] Southampton Oceanography Center, Southampton, UK

Abstract

A new model-based method of determining the surface fluxes of heat and freshwater that are needed to force ocean models is presented. In contrast to deriving the fluxes from a simulation with a restoring surface boundary condition, the new method determines the fluxes as a residual within the framework of physically realistic and natural boundary conditions on the sea surface temperature (SST) and sea surface salinity (SSS). The fluxes are computed (diagnosed) in such a way that an ensemble average of the model-simulated annual cycles of SST and SSS match the observed climatological annual cycles of SST and SSS, respectively. The surface boundary condition on the SST implicitly includes a net radiative flux (diagnosed) and a physically realistic heat exchange with the atmosphere (restoring flux), while the boundary condition on the SSS is the real freshwater flux (diagnosed) as proposed by Huang (J. Phys. Oceanogr., 33 (1993) 2428). Apart from being based on physically realistic surface boundary conditions, the advantage of the method is that it results in a realistic model simulation of the observed annual cycle of SST and SSS with no artificial damping of surface watermass fronts. The resulting heat fluxes and freshwater sources are realistic if the observed climatological data and model internal physics are accurate. The performance of the method is demonstrated using the DieCAST ocean model adapted to the Mediterranean Sea where the obtained model fluxes are compared with observations.
© 2004 Elsevier B.V. All rights reserved.

Keywords: Ocean modeling; Surface buoyancy fluxes; Mediterranean Sea

1. Introduction

For the past 30 years ocean modelers have been struggling with the problem of determining the surface fluxes of heat and freshwater that are needed to force ocean models. Because these fluxes depend on small air–sea temperature and humidity differences, direct measurements of the heat fluxes and freshwater sources with coverage and accuracy required for an ocean model is extremely difficult over the vast world ocean. Although the required fluxes are readily com-

* Corresponding author. Tel.: +34-9-71-611732.
E-mail address: v.fernandez@uib.es (V. Fernández).

puted from operational, data assimilating, numerical weather prediction models, such models do not need, or yet produce, these data with the accuracy and mesoscale resolution needed by ocean models.

Thus, one must use more accurately known ocean surface data, primarily the sea surface temperature (SST) and sea surface salinity (SSS), to infer the required surface boundary fluxes. One possible approach in this regard is to use fluxes that have been diagnosed from a preliminary model simulation that was forced by a surface restoring condition on both SST and SSS (Myers and Haines, 2000). Another quite common approach is to use only surface restoring with constant restoring coefficients (Beckers and MEDMEX, 2002; Wu and Haines, 1998); with time-dependent parameterization of the restoring coefficient (Artale et al., 2002), or air–sea heat flux bulk formulae with meteorological data and sea surface temperature from the model (Roussenov et al., 1995; Castellari et al., 1998, 2000). Thus, although some notable progress has been made since Haney (1971) to improve surface restoring-type boundary conditions on the SST (e.g., Rahmstorf and Willebrand, 1995; Pierce, 1996), serious fundamental problems still remain. The basic problem with restoring-type boundary conditions is that by restoring to climatological SST, one cannot produce a realistic annual cycle of SST without excessively damping internal variability (fronts and eddies). This problem has been recently analyzed in detail by Killworth et al. (2000). Most unsettling from a physical point of view is the fact that surface restoring boundary conditions are clearly inappropriate for salinity. This is because the freshwater flux, primarily precipitation minus evaporation, is not physically linked to surface salinity anomalies. The particular problem of salinity was recognized by Huang (1993) who developed the natural boundary condition, i.e., the direct use of freshwater flux, and successfully implemented it in the Bryan–Cox (Bryan, 1969) rigid-lid model. A complete analysis of the different boundary conditions on SSS, including the natural boundary condition of Huang (1993), is presented by Roullet and Madec (2000).

In the present paper, we describe a procedure for diagnosing the climatological heat flux and freshwater sources while using physically correct boundary conditions on the SST and SSS. The performance of this procedure is demonstrated in the DieCAST model

applied to the Mediterranean Sea. The adaptation of the DieCAST ocean model to the Mediterranean Sea is described in Section 2, while the details of the surface boundary conditions for heat and freshwater flux are given in Section 3. Results demonstrating the performance of the approach are given in Section 4, and a brief summary and discussion is given in Section 5.

2. Adaptation of the DieCAST ocean model to the Mediterranean Sea

The Mediterranean Sea is a nearly closed region having areas of significant long-term average freshwater sink (evaporation (E) larger than precipitation and runoff (P), primarily in the eastern basin), and regions of strong heat loss to the atmosphere (e.g., The Adriatic Sea or the Gulf of Lions). Thus, it is an ideal place to explore surface buoyancy flux issues.

2.1. Numerical approach and resolution

The DieCAST Ocean Model (Dietrich, 1997) used in this study is a z-level, rigid-lid, primitive equation model using a non-staggered control volume grid layout (Dietrich and Ko, 1994). Except for the hydrostatic vertical pressure gradient, all significant numerical approximations, including horizontal and vertical advection, are computed using fourth-order accuracy except in zones adjacent to boundaries where conventional second-order accuracy is used.

A fundamental attribute of control volume-based models is that the predicted quantities are control volume averages, while face-averaged quantities are used to evaluate fluxes across control volume faces. Conversions between the control volume averages and face averages are needed. In the DieCAST model, these are computed using fourth-order accurate approximations (Sanderson and Brassington, 1998). A modified incompressibility algorithm (Dietrich, 1997) further reduces numerical dispersion errors. The horizontal baroclinic pressure gradient and all advection terms are evaluated using fourth-order accurate approximations.

Horizontal resolution is the same in both the longitudinal (λ) and latitudinal (ϕ) directions, with $\Delta\lambda = 1/8°$ and $\Delta\phi = \Delta\lambda \cos(\phi)$, thus making square

horizontal control volume boundaries. Vertical resolution is variable, with 30 control volume layers. The top layer control volumes are 10.3 m thick. Control volume thickness increases smoothly to the model's deepest bottom control volume face at 2750 m. ETOP05 bathymetry is thus truncated at depth 2750 m. Except by this truncation, the model bathymetry it is not filtered or smoothed in any way. The model time step is 15 min.

2.2. Model parameters and boundary conditions

Lateral viscosity and diffusivity are specified constants of 10 m^2 s^{-1}. The vertical viscosity and diffusivity are based on Pacanowski and Philander (1981), as modified by Staneva et al. (2001), with background vertical viscosity and diffusivity set at near-molecular values (0.01 and 0.002 cm^2 s^{-1}, respectively).

We use monthly mean wind stress re-analyzed from 10 m wind output from ECMWF, as chosen for the Mediterranean Sea Models Evaluation Experiment (Beckers and MEDMEX, 2002). MODB monthly climatology of sea surface temperature and salinity (Brasseur et al., 1996) is used to determine the

heat and the freshwater sources in the surface layer. These are computed using the model-based method described below (Sections 3.1 and 3.2). As shown there, the method produces no intrinsic error in the phase or amplitude of the annual cycle at the surface, and it does not damp surface watermass fronts.

The only open boundary is the Strait of Gibraltar. Everywhere else, free-slip lateral boundary conditions are used (e.g., Hughes, 2000). All bottom dissipation is represented by conventional nonlinear bottom drag with drag coefficient 0.002. Lateral and bottom boundaries are thermally insulated.

2.3. Strait of Gibraltar

The only open boundary condition in the model is the Strait of Gibraltar. An upper layer inflow of 0.80 Sv Atlantic water is specified in the upper 105 m, with the velocity itself taken to be similar to recent observations (Baschcek et al., 2001). The specified inflow vertical shear is supergeostrophic because the climatology gives far too little geostrophic transport; the Gibraltar inflow is actually thought to be significantly supergeostrophic (e.g., Viudez, 1997). The inflow salinity and temperature are based on the MODB
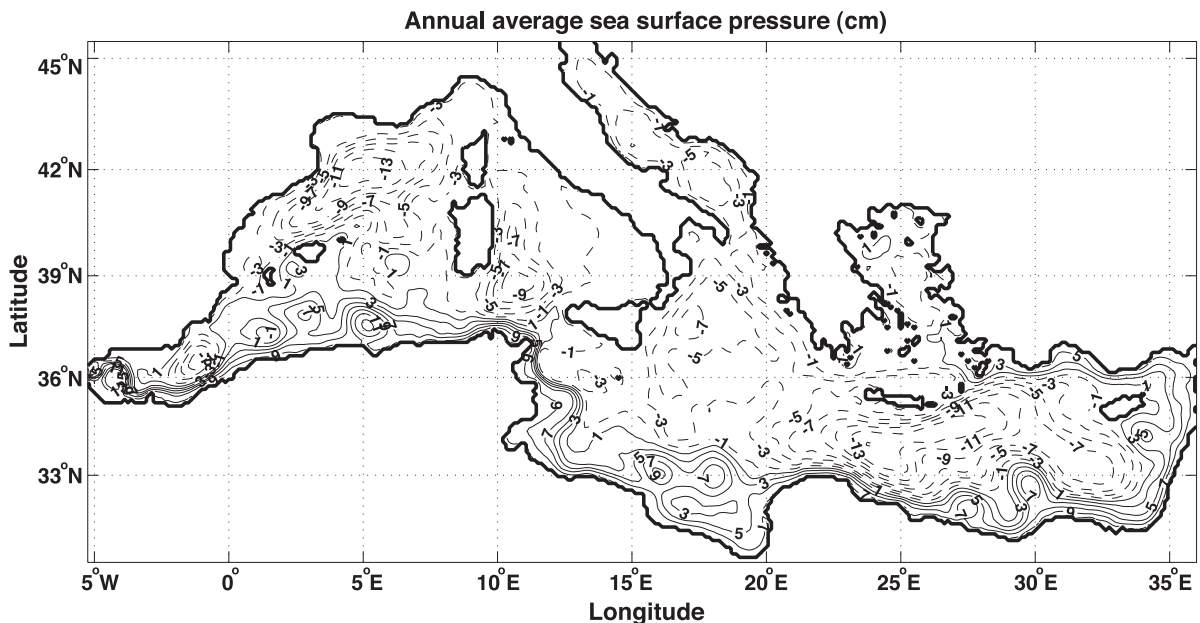

Fig. 1. Annual average sea surface pressure (in equivalent cm) for the 16th year of simulation.

summer climatology (Brasseur et al., 1996). Outflow takes place between 105 m and the model bottom. It is determined using an upwind approximation, but is modified by a meridionally uniform increment at each time step to maintain a net volume inflow through the strait equal to the computed net surface volume sink $(E - P)$. With the actual inflow and outflow Gibraltar conditions we reproduce a correct first Alboran gyre in the Alboran Sea (Fig. 1). We should note here that the circulation in the Alboran Sea is very sensitive to changes in the Gibraltar conditions, but in this study we do not take into account the variability in the inflow or changes in the interface between inflow and outflow in the Strait of Gibraltar.

3. Model-determined surface fluxes

3.1. Surface heat flux

In the surface heat flux treatment of our DieCAST Mediterranean Sea model, an array $Q_{m+1/2,n}$, where m is the month ($m = 0, \ldots, 11$) and n is the year, gives the temperature change per time step that is added to the top layer in addition to the effects of advection, diffusion, and a physically realistic restoring to the observed SST. By construction, this change, when added to the model's simulated internal heat transport dynamics, keeps the multi-year ensemble average model SST on track with the climatological observed SST. This temperature change represents the surface layer external heat source, which, in the presence of a physically realistic surface restoring, will keep the model on track with climatology. We first present the surface thermal boundary condition, and then describe how $Q_{m+1/2,n}$ is determined and used in the model.

In a given model time step, from t to $t + dt$, occurring between the center of month m and the center of month $m + 1$, the surface layer temperature T is updated as follows:

$$T_{t+dt} = T_t + A_{t+dt/2} + Q_{m+1/2,n} + T^{\text{nudge}}_{t+dt/2}, \qquad (1)$$

where $T^{\text{nudge}}_{t+dt/2} = (dt/\tau_T)(T^c - T_{t+dt/2})$. Here, n is the year; A represents the advection and diffusion terms; T^{nudge} is the nudging toward surface climatology; T^c is the surface climatology interpolated to the present time; and τ_T is the time scale for nudging toward climatology.

In Eq. (1), $Q_{m+1/2,n}$ represents the temperature change during one time step due to the non-restoring part of the model-determined monthly climatological surface heat flux. The T^{nudge} term represents an instantaneous physical damping of model sea-surface temperature anomalies to the atmosphere (Haney, 1971). Thus, τ_T should be chosen to emulate a physically realistic damping time. Pierce (1996) has examined the restoring time scales and suggest a realistic coupling coefficient ranging from 40 W/(m^2 °C) for small scales to 2 W/(m^2 °C) for very large scales (see also Rahmstorf and Willebrand, 1995). Seager et al. (1995) suggest to use a value of 10 W/(m^2 °C). In our case, we have a value of 16 W/(m^2 °C) which corresponds to $\tau_T = 30$ days (for our Δz of 10.3 m).

Eq. (1) presents the surface thermal boundary condition used in the model. The surface thermal forcing is the sum of a climatological surface temperature change Q plus a small, physically realistic surface restoring, T^{nudge}. While T^{nudge} is directly computed at each time step in the model, Q is computed iteratively once each month. We now turn to the determination of Q.

Let us initialize the upper layer temperature in the model, T at $t = 0$ (taken to be 15th January), by the climatological surface layer temperature in January ($m = 1$).

$$T_0 = T^c_1 \qquad (2)$$

Since $Q_{m+1/2,n}$ is determined by iteration it must be initialized for the first year ($n = 1$). This can be done by using any reasonable guess for the surface heating rate. Noting that the basin-scale mean horizontal advection is negligible for a nearly closed basin like the Mediterranean Sea, a reasonable initialization for Q is:

$$Q_{m+1/2,0} = (T^c_{m+1} - T^c_m)/N, \qquad (3)$$

where N is the number of time steps per month. The initial surface temperature change given by Eq. (3) will be the correct value wherever the model SST is determined entirely by the surface heat flux. That is, wherever advection and mixing are negligible (or cancel each other). With the above choices for T_0 and $Q_{m+1/2,0}$, it can be seen from Eq. (1) that T will follow climatology (T^c), and thus T^{nudge} will be small, except where T is influenced significantly by such advection or mixing.

At the center of each month, Q is modified (updated) for use during the following year according to the following two steps:

Step 1.

An auxillary variable $q_{m+1/2,n}$ is calculated from the model top layer data:

$$q_{m+1/2,n+1} = Q_{m+1/2,n} + a_{m+1/2,n}, \tag{4}$$

where

$$a_{m+1/2,n} = [T_{m+1}^c - T + \Sigma T^{\text{nudge}}]/N. \tag{5}$$

In Eq. (5), T_{m+1}^c is the climatological SST of month $m+1$, T is the (instantaneous) model SST at the center of month $m+1$, and ΣT^{nudge} is the sum of the nudgings from the center of month m to the center month $m+1$. Next year's heat-flux $Q_{m+1/2,n+1}$ is computed from q in Step 2 below. The temperature difference $T_{m+1}^c - T$ in Eq. (5) represents the amount by which the effective heating in the top layer due to all processes (nudging, advection, diffusion and $Q_{m+1/2,n}$ during the previous 30 days) failed to produce the climatological temperature of month $m+1$. Thus, $a_{m+1/2,n}$ is the amount by which Q should be changed in order to force the temperature misfit $T_{m+1}^c - T$ to be zero, assuming everything else remains the same. This altered value of Q is given by $q_{m+1/2,n+1}$ in Eq. (4). But of course everything will not remain the same the following year because an altered Q will to some extent change the advection, diffusion and nudging values. Most importantly, since the SST misfit is computed using the instantaneous model temperature at the middle of the month, the adjustment $a_{m+1/2,n}$ and hence $q_{m+1/2,n+1}$ in Eq. (4) will experience year-to-year fluctuations simply because of the inherent natural variability of T; i.e., because of transient upper ocean fronts. Thus, to obtain an accurate model-based Q-climatology, one should average this year's value of Q with those of previous years. To do this, we compute $Q_{m+1/2,n+1}$ as an ensemble average of q over the total amount of years that the model has run according to

Step 2.

$$Q_{m+1/2,n+1} = \left(\frac{1}{n+1}\right) \sum_{j=1}^{n+1} q_{m+1/2,j}, \tag{6}$$

where $q_{m+1/2,1} = Q_{m+1/2,0} = [T_{m+1}^c - T_m^c]/N$. We have implicitly assumed $a_{m+1/2,0}=0$ in the absence of a

reasonable initial estimate for $a_{m+1/2,n}$. Such initial estimate is rather arbitrary, because the converged ensemble Q is independent of the initial guess.

It is instructive to consider the method from the start of a simulation. With no nudging, the first 30 days (from the center of January to the center of February) result (from Eq. (1) along with initial conditions (2) and (3)), is:

$$\begin{aligned} T_{30 \text{ days}} &= T_0 + T_{m+1}^c - T_m^c + \sum A \\ &= T_m^c + T_{m+1}^c - T_m^c + \sum A \\ &= T_{m+1}^c + \sum A, \end{aligned} \tag{7}$$

where ΣA is the sum of the changes caused by advection and diffusion during these 30 days. If $\Sigma A = 0$, the result is exact ($T_{30 \text{ days}} = T_{m+1}^c$). Later we will see that even with advection in a real application to the Mediterranean Sea, the annual cycle is accurately reproduced. A second, highly desirable property of the present approach is that it does not damp surface fronts unrealistically. In the absence of nudging, or in the presence of realistically weak nudging, the model can sustain surface fronts. Temporal fluctuations in the simulated SST, produced by the transient nature of such fronts, only slightly influence the surface heat flux locally. This occurs specifically through the T^{nudge} term which tends to average to zero over time. As shown in Appendix A, the major development of the Q-field from its initial annual cycle $Q_{m+1/2,0}$ occurs within the first few years of the simulation as a result of seasonally persistent advection/mixing at the places where such mixing/advection is significant.

The above surface heat flux boundary treatment may be summarized as follows: the model is thermally forced at the surface by a specified monthly mean heat flux, $Q_{m+1/2,n}$, and by a realistically weak restoring to the monthly climatological SST, T^{nudge}. This is the surface thermal boundary condition as expressed in Eq. (1). The monthly mean heat flux Q is computed within the model by iteration. Starting with a good estimate for the first year (Eq. (3)), in subsequent years Q is replaced by an ensemble average of adjusted fluxes (Eq. (6)) constructed so that the model-simulated ensemble average annual cycle of SST closely follows the observed climatological SST. It follows therefore that although T^{nudge} may be

different from zero at any given time, its ensemble average will vanish. Thus, in this formulation, the long-term ensemble average heat flux at the sea surface is entirely contained in Q. Additional details are given in Appendix A.

3.2. Freshwater flux

As stated earlier, a surface restoring condition for salinity is not appropriate. The correct boundary condition for salinity at the surface is the natural boundary condition for the source (sink) of freshwater (Huang, 1993). Our salt-material-conserving approach, which includes surface freshwater volume sources, consists of removing (evaporating) or depositing (rainfall and runoff from rivers) freshwater at the surface at a rate such that the salinity of the top layer remains on track with climatology. This means modifying the surface normal velocity relative to the surface (air–sea interface). Thus, the model's "rigid lid" is actually slightly porous, with a non-zero vertical velocity representing the freshwater flux (Huang, 1993). In the case of an upward flux, the removed liquid is salt-free even though the ocean water contains salt. The fact that the relative vertical velocity applies only to freshwater, and does not include salt or any other significant material (ignoring CO_2 exchanges, etc.), is used in the surface flux condition. This is a macroscale representation of a molecular scale process in which the water molecules have a mean vertical drift relative to the sparsely distributed salt molecules. Such a vertical velocity must occur in the long-term mean in the absence of mean sea level changes. The (evaporating) liquid water changes phase as fast as it reaches the surface. This means that the sea surface will remain at a given level only if sea water converges to the location from within the liquid. Such convergence allows evaporation to occur while applying the rigid-lid approximation. In general there must be such horizontal convergence of sea water into regions where the long-term average $E - P$ is positive because there are no long-term mean changes in sea level.

Recognizing that direct observations of evaporation rates do not exist over large bodies of water, and reliable rainfall information is not available away from land, the surface freshwater flux, like the heat flux, is model-determined. The model uses the natural

boundary condition on SSS, and a model-determined monthly mean surface vertical velocity, W^{top}, to model $E - P$ effects as advocated by Huang (1993). The sign convention is such that $W^{top} = P - E$, in units of m/s, represents the net downward flux of freshwater into the ocean topmost layer. Actually, the laterally inward flux of freshwater at lateral boundaries (fresh river sources, R) is also implicitly included in W^{top} (see below). Analogous to the method used for temperature in Eq. (1), the surface layer salinity is advanced each time step as follows:

$$S_{t+dt} = S_t + A^S_{t+dt/2}, \qquad (8)$$

where $A^S_{t+dt/2}$ represents the advection and diffusion terms for salinity in the model top layer. Note that there is no salt flux across the top cell face in Eq. (8). However, when W^{top} is non-zero, the surface cell salt content is affected by an induced net divergence or convergence of salty water through the sides and bottom of the surface cell which is accounted by the term A^S in Eq. (8).

Like the heat flux Q, the freshwater flux W^{top} represents a monthly mean quantity and is used (held constant) throughout the month. At the center of each model calendar month (m) W^{top} is computed by iteration in a two-step procedure that is similar to the method used to determine Q:

Step 1.

$$w^{top}_{m+1/2,n+1} = W^{top}_{m+1/2,n} + b_{m+1/2,n}, \qquad (9)$$

where

$$b_{m+1/2,n} = (\Delta z / \tau_s)(S - S^c_{m+1})/S^{avg}. \qquad (10)$$

Here: n is the present model year; W^{top} represents an instantaneous value of the surface vertical velocity; $W^{top}_{m+1/2,n}$ is the surface vertical velocity (positive for downward motion) between the middle of month m and the middle of month $m + 1$ as determined for year n during previous model years; Δz is the thickness of the top layer; $b_{m+1/2,n}$ is an adjustment to W^{top}; S is the model top layer salinity at the center of the month $m + 1$; S^c_{m+1} is the climatological salinity of month $m + 1$; S^{avg} is preferably the average of the model top layer salinity during the previous 30 days, but the instantaneous value at the center of the month may be used as we do; and τ_s is the time over which the salinity misfit ($S - S^c_{m+1}$) is to be brought to zero by

the surface freshwater fluxes. We use $\tau_s = 30$ days. Unlike in the temperature tendency (Eq. (1)), there is no surface restoring of salinity. We use only the salinity misfit $(S - S_{m+1}^c)$ to help diagnose the adjustment to the freshwater flux, b, in Eq. (10). The freshwater flux itself is computed as in Huang (1993) using a running mean of W^{top}:

Step 2.

$$W_{m+1/2,n+1}^{top} = \frac{1}{n+1} \sum_{j=1}^{n+1} w_{m+1/2,j}^{top}. \quad (11)$$

As computed above, W^{top} will effectively include a representation of freshwater input from rivers. Near river ports the climatological surface salinity S^c is comparatively small, and this tends to produce positive values of b and W^{top}, as can be seen from Eqs. (9) to (11). Numerically, it does not matter whether freshwater enters through a lateral face (river input) or the top face of the model control volume.

Similar to the initialization of the heat flux in Eq. (3), a reasonable initialization for W^{top} is:

$$W_{m+1/2,0}^{top} = \frac{\Delta z}{\tau_S} \left(\frac{S_{m+1}^c - S_m^c}{\frac{1}{2}(S_{m+1}^c + S_m^c)} \right). \quad (12)$$

To understand the physical interpretation of the method, consider a situation in which water particles at the surface in the model are being advected into a region with comparatively low climatological salinity, so that on average $S - S^c > 0$. Then from Eqs. (9)–(11), W^{top} will tend to be positive provided the salinity advection persists so as to keep $S - S^c > 0$. Since $W^{top} > 0$ implies sinking motion, it means $P - E > 0$ which implies a freshwater source. In the model, it does not matter whether the relatively small S^c, and the positive $P - E$, has resulted from excessive rainfall or from river inflow. The result ($W^{top} > 0$) is the same. Freshwater is added to the surface layer at this location. This represents a volume source of freshwater at the surface which is compensated by a horizontal divergence of (salty) water in the column, resulting in a decrease of salinity in the top layer. Again, it is necessary only for S to exceed S^c on average (not every year), because W^{top} is computed as an ensemble average (Eq. (11)). Thus, fluctuations in $S - S^c$ as may occur in transient frontal regions are averaged out, so only the model climatological S, not its instantaneous S, is constrained toward S^c.

As described above, the addition (or removal) of a given amount of freshwater to (from) the top of the sea ($W^{top} \neq 0$) affects the salt budget because the water that is added to (or taken from) the sea has a different salinity (namely zero) than the sea itself. In the same way, the added or subtracted water will also affect the heat and momentum budget if the temperature and momentum of the water crossing the sea surface is different from that of the sea. In our implementation of the natural boundary conditions, we assume that incoming water has $S = 0$, $T = T_s$ and $(u,v) = (0,0)$; while outgoing water has $S = 0$, $T = T_s$ and $(u,v) = (u_s,v_s)$ where subscript s indicates a model surface value. Thus, "entering" water brings a deficit of salt and momentum (but no deficit of heat) while 'leaving' water leaves only salt behind (no heat or momentum). These assumptions could obviously be changed upon further study.

4. Results

In this section we will present the results of applying the above boundary conditions to a simulation of the Mediterranean Sea. The model has been integrated for 16 years, starting from a winter climatological state and with zero velocities. Although the main focus in this study is on the upper ocean temperature and salinity fields that are directly influenced by the new boundary conditions, the simulated general circulation is also important. The geostrophic surface circulation as shown by isolines of surface pressure is representative of the general circulation of the upper ocean. In Fig. 1, we show the annual average surface pressure for the last year of the model run. The basic features of the observed mean surface circulation are reproduced in the simulation: the Algerian and the northern current in the western basin; the gyres in the Adriatic Sea and the general cyclonic circulation in the eastern basin. Thus, the mean surface circulation obtained in the present simulation with non-restoring boundary conditions is qualitatively comparable with other model results obtained using different surface forcing approaches (e.g., Beckers and MEDMEX, 2002) and with the results from a previous DieCAST model simulation with a standard restoring boundary condition (Fernández et al., in press).

As described in Section 3, the surface fluxes of heat and freshwater are computed in such a way that, on average, the model surface temperature and salinity follow the prescribed climatology. In order to verify that the method of computing the fluxes is working properly, we will show the model-simulated temperature and salinity fields, and compare them to the climatology. Although a more complete evaluation of the Mediterranean Sea model under the non-restoring boundary conditions is left for a future study, we will show here the model-determined surface heat and freshwater fluxes and compare them with estimates of these fields from observations. This comparison is more an evaluation of the model, including its forcing, than it is of the method used to compute the surface fluxes. For example, regions where the model fluxes and observed fluxes are very different show where either the underlying model physics or the observed fluxes are in error.

Fig. 2 shows the convergence of the annual basin averaged vertical profile of temperature and salinity towards a steady vertical profile, indicating that the model is in equilibrium in 16 years of integration and considering that there is no deep water production (lack of synoptic events in the model forcing). In Fig. 2 we can also see the smallness of the drift of the model deep horizontal mean temperature and salinity from its initial climatological values, indicating that the model total vertical mixing (resolved plus parameterized) is
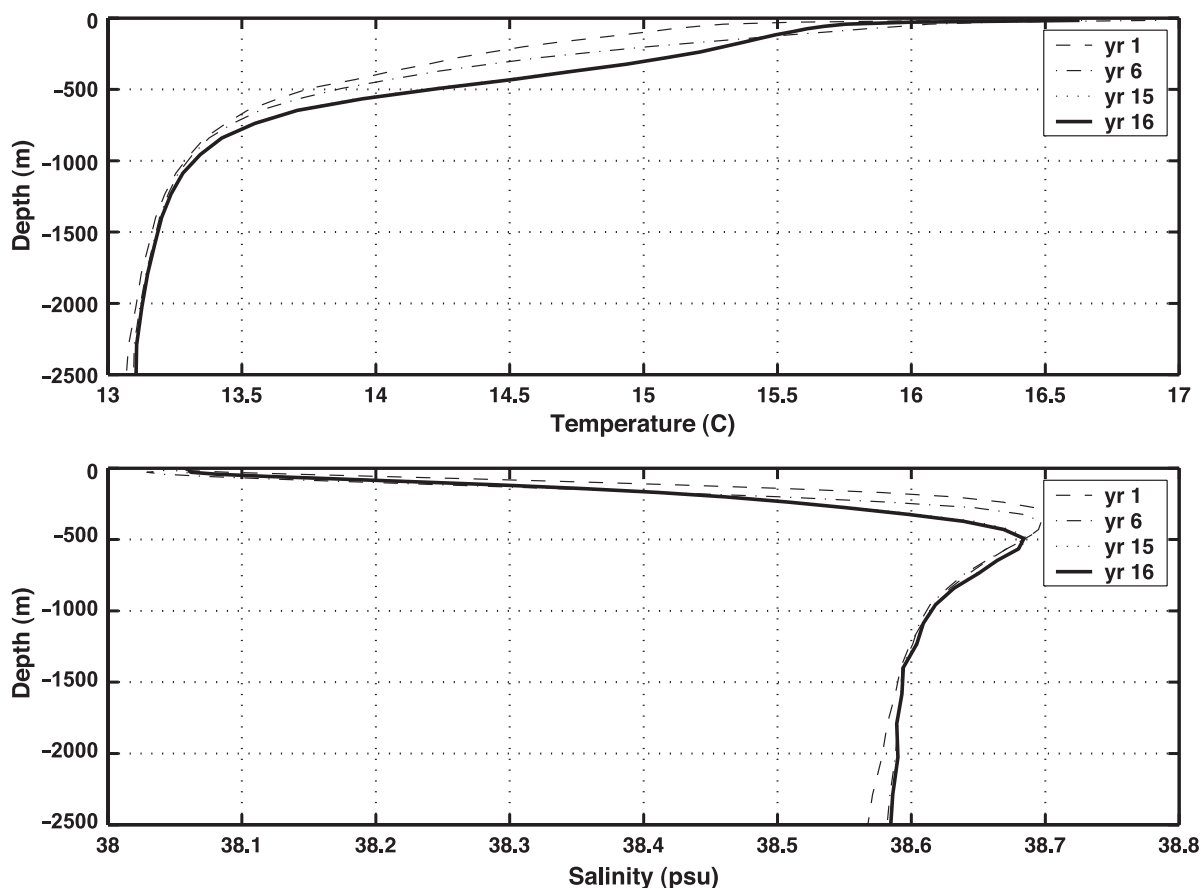

Fig. 2. Time evolution of the annual average profile, over all model grid points, of temperature and salinity from the initial climatological winter conditions (year 1) to the last year of simulation.

reasonably accurate. This drift presumably could be reduced further by a careful refinement of the Pacanowski–Philander vertical mixing scheme used in the model.

Figs. 3 and 4 show the model annual average surface temperature and salinity, respectively, along with the corresponding climatological fields. The model mean surface temperature and salinity values and structures resemble quite well the observed climatology, as expected by construction. However, as we have remarked throughout this paper, the proposed model surface boundary conditions do not damp surface fronts of temperature or salinity that can appear naturally in the model. An example of this

can be seen in Fig. 5 where the model shows a tight surface salinity front in the Balearic Sea, separating saltier waters in the north from fresher waters to the south. This front is not present in the climatological sea surface salinity, therefore indicating that an instantaneous model front is not being artificially damped by the computed surface fluxes. The tight surface salinity front that appears at 6E and 40N in year 16 of the simulation (Fig. 6), which is not present at the same time in year 15, is another example of a transient surface structure that appears in the model. These results demonstrate the ability of the model, with such diagnosed fluxes, to represent mesoscale structures in the upper ocean.
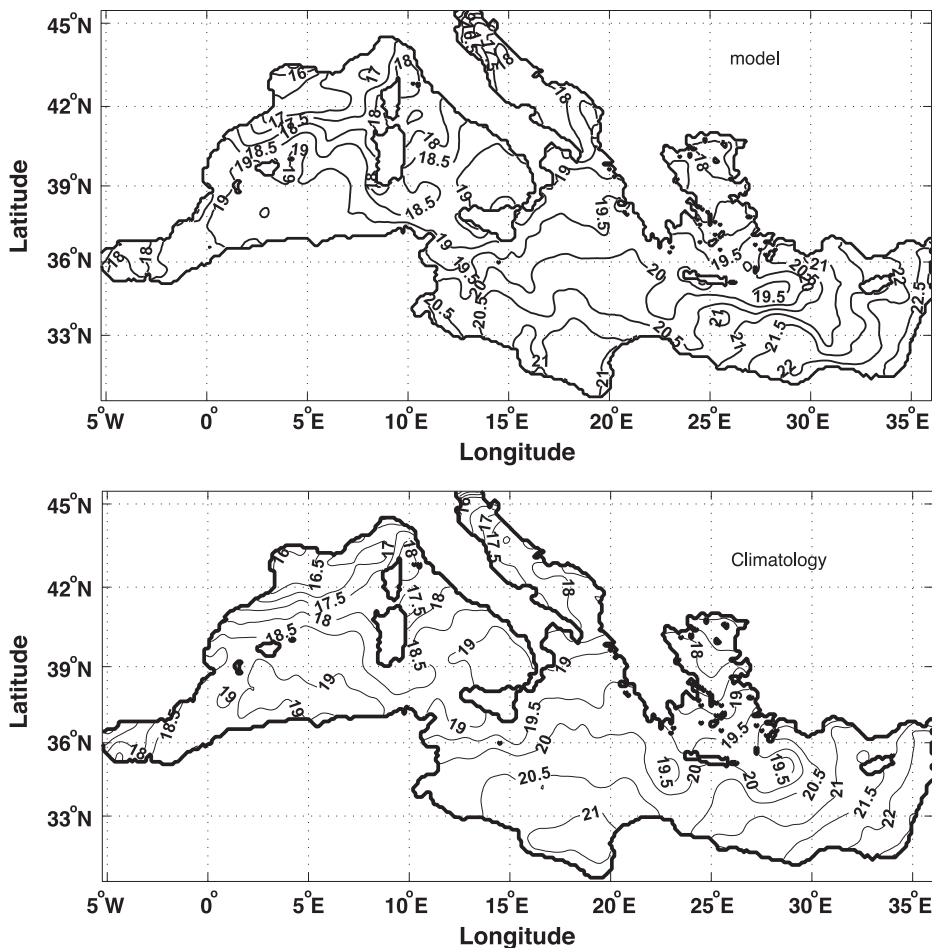

Fig. 3. Map showing the horizontal distribution of the annual average model surface temperature and the corresponding annual average surface climatological temperature.
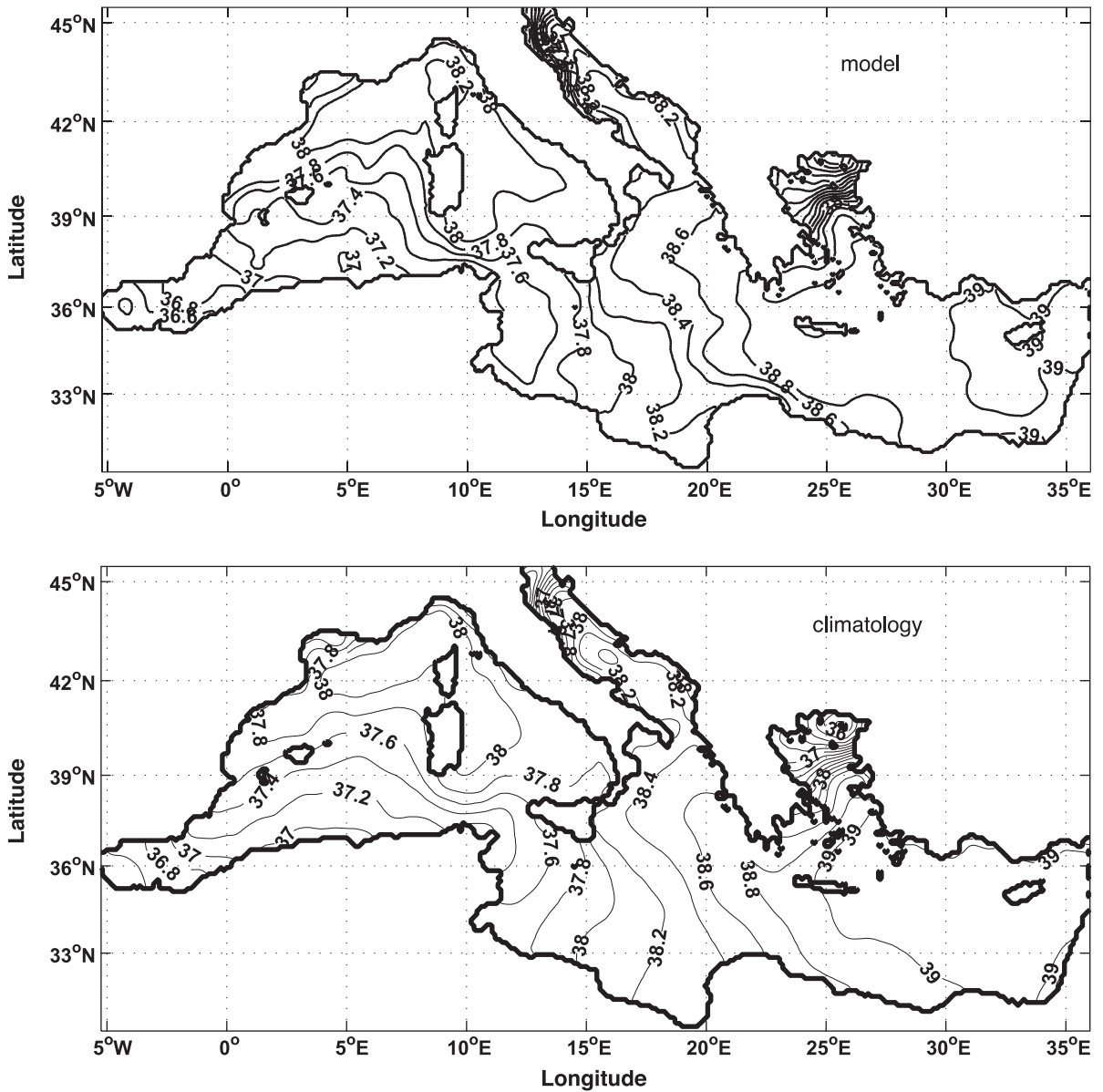
Fig. 4. Same as Fig. 3 but for the surface salinity.

Fig. 7 shows the annual cycle of the horizontally averaged model temperature and salinity in the topmost layer along with the corresponding climatological data. Horizontal averaging removes the effects of transient eddies and thus is qualitatively representative of an ensemble model annual cycle at a point. At the end of the integration, the annual cycle of temperature is largely converged to the climatological annual cycle. As noted in the previous section, there is almost no phase difference between the observed and simulated annual cycle. The almost imperceptible phase lag, with the simulated temperature lagging the observed temperature, is due to the weak restoring (T^{nudge} in Eq. (1)) included in the boundary condition.
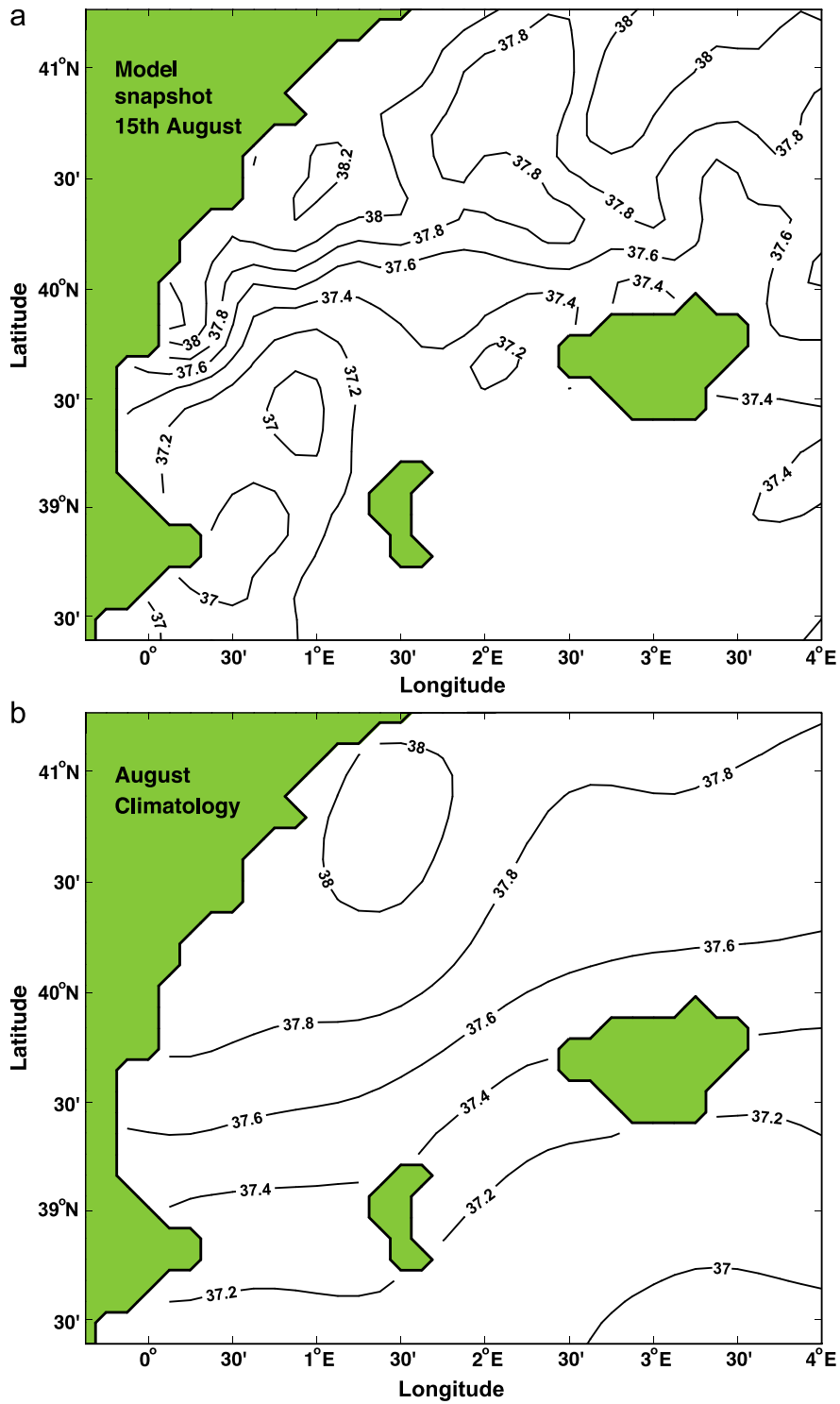
Fig. 5. (a) Model snapshot of the surface salinity on 15 August of year 16; (b) Sea Surface Salinity climatology corresponding to the month of August.
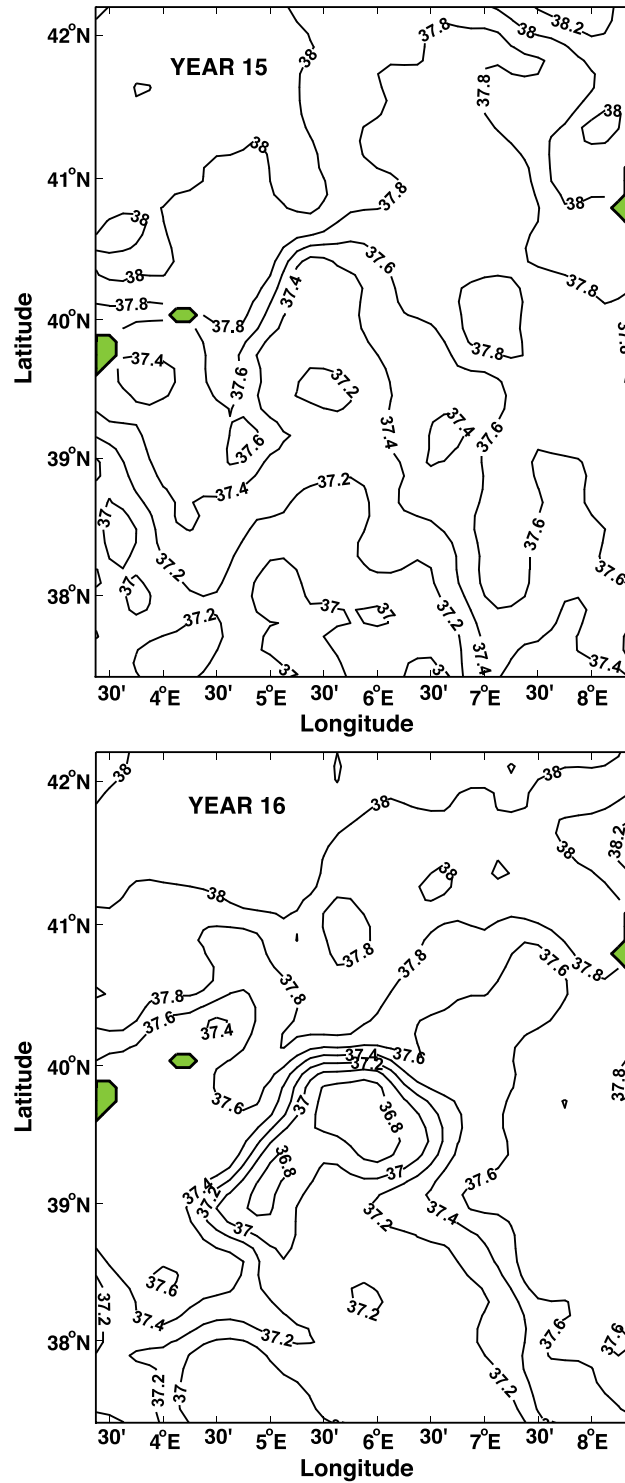
Fig. 6. Two model snapshots of surface salinity on 15 November of two consecutive model years.
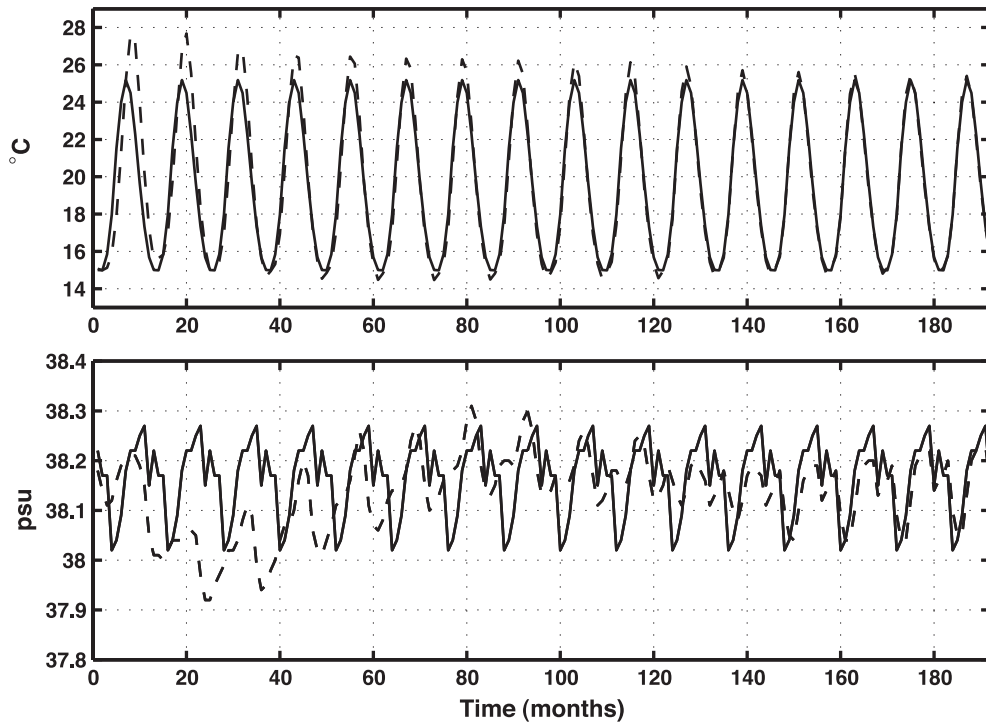
Fig. 7. Time evolution of the horizontally averaged model temperature and salinity in the top-most layer (dashed) along with the corresponding observed climatological data (solid).

If surface restoring (only) were used to compute the heat flux there would be a bigger time lag as noted by Killworth et al. (2000). The convergence to climatol-ogy is slower for salinity than it is for temperature. This is not surprising because there is no restoring at all in the natural boundary condition on freshwater.
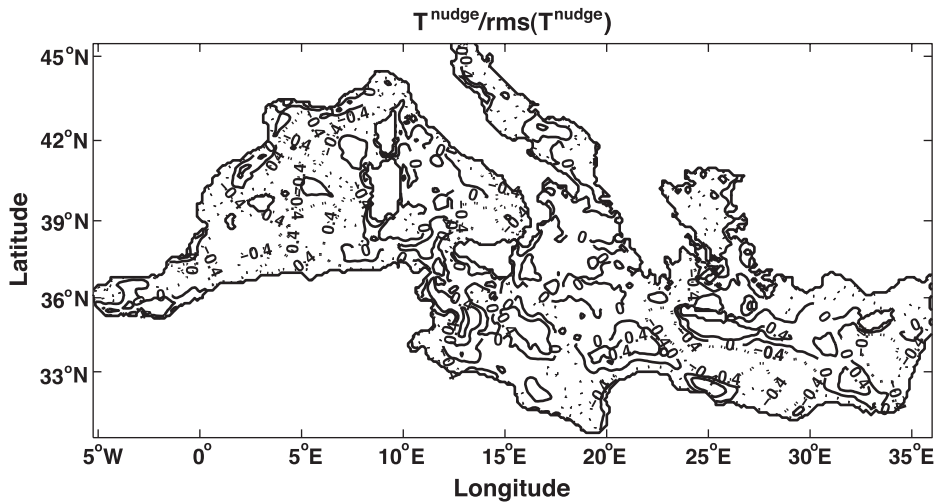

Fig. 8. Horizontal distribution of the average T^{nudge} divided by the average of the rms of T^{nudge} based on three years of simulation (years 14, 15 and 16). The contour interval is 0.4.

Since the external surface thermal forcing is the sum of two different terms (T^{nudge} and Q in Eq. (1)), we first examine the relative contribution of each one of these terms to the total heat flux. The nudging term

(T^{nudge}) can be important locally in time in regions affected by transient temperature fronts where T differs from T^{c} (due to the inherent natural variability of surface T). However, in an ensemble sense, the
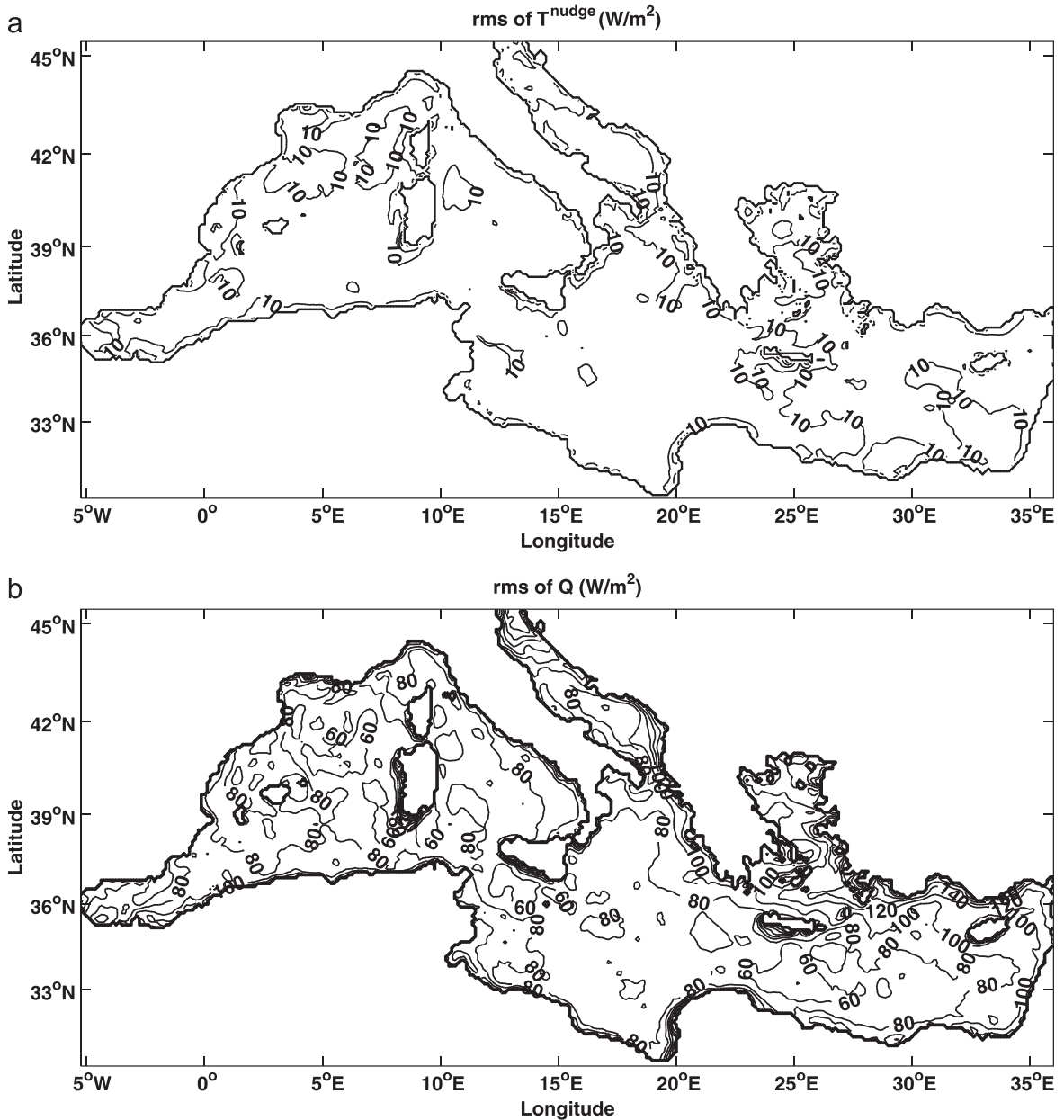

Fig. 9. Horizontal distribution of (a) rms of the restoring term T^{nudge}; and (b) rms of model-determined heat flux Q. Both units are in W/m^2 and the contour interval is 10 in panel a, and 20 in panel b.

contribution of T^{nudge} to the total heat flux should be small. We demonstrate this by showing in Fig. 8 that the ratio of the ensemble average T^{nudge} to the rms of T^{nudge} (over the last 3 years of the simulation) is everywhere smaller than 1. To better quantify the relative contribution of T^{nudge} to the total heat flux, we show in Fig. 9, the horizontal distribution of the rms values of T^{nudge} and Q over the last 3 years of simulation. Note that the variability induced by T^{nudge} is much smaller than the variability given by the total heat flux (9 W/m^2 vs. 86 W/m^2).

We now compare the model determined fluxes with an estimation of air–sea fluxes computed from observations. The observation based dataset employed is the recently developed Southampton Oceanography Centre (SOC) flux climatology (Josey et al., 1999). The SOC fluxes have been obtained from marine meteorological observations for the period 1980–1993 using various semi-empirical flux formulae (see Josey et al., 1999, for details of the method). For our study, we use a revised version of the original SOC fields for the Mediterranean Sea. The revisions consist of improved estimates of the longwave and shortwave flux components which have been calculated using formulae developed specifically for the Mediterranean basin. The revised longwave flux has been estimated using the formula of Bignami et al. (1995) which provides more accurate estimates in the Mediterranean than the formula originally employed for the global SOC climatology. In addition, the shortwave flux has been corrected for the effects of aerosol attenuation, which are significant for the Mediterranean, according to the method of Gilman and Garret (1994).

We show in Fig. 10 the annual cycle of the horizontally averaged model determined fluxes (over year 16 of the simulation) along with the corresponding annual cycle of the SOC climatology. There is a reasonable agreement for the heat flux annual cycle (Fig. 10A). The maximum heat loss (upward flux) occurs in the model between the months of December and January while in the SOC climatology this maximum takes place in the month of December. The maximum heat gain occurs between the months of May and June in the model and in June in the SOC climatology. However, the amplitude of the seasonal cycle in the model is a bit smaller than the observed amplitude. The lack of
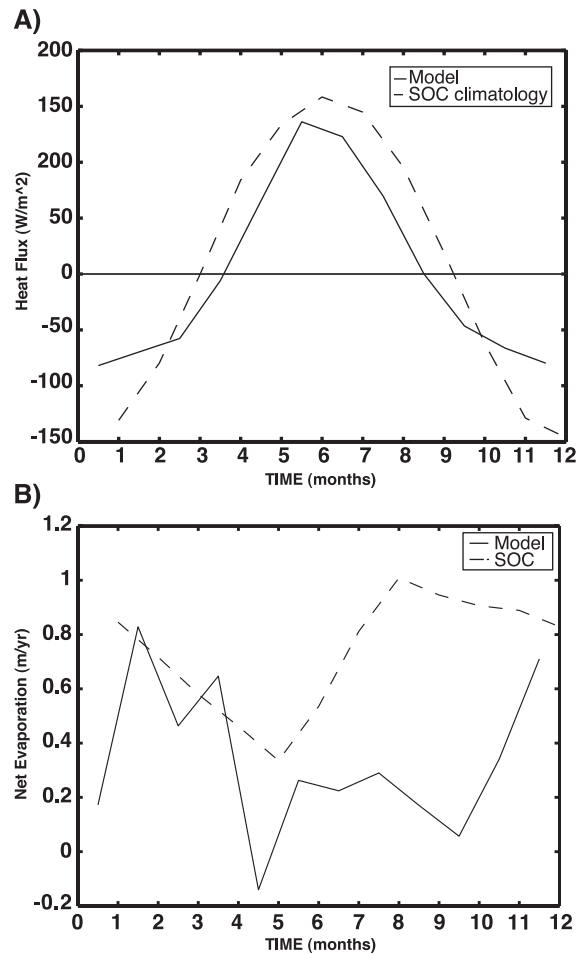

Fig. 10. Annual cycle of (A) horizontally averaged surface heat flux (in W/m^2); and (B) net evaporation ($E - P$, in m/year).

synoptic events in the model forcing can account for this difference in the domain averaged annual cycles. On the other hand, the seasonal cycle of W^{top} (which is, by construction, the surface freshwater source that keeps the model simulation on track with climatology) does not match so well with the observations (Fig. 10B). The main difference is that while evaporation exceeds precipitation ($E - P > 0$) for all months in the observations, in the model there is a net precipitation between April and May. A possible reason for this is the freshwater runoff in spring, which is included in the model but not in the SOC climatology. We can say, however, that there is a similar order of magnitude for both freshwater fluxes (model and observed).

The annual mean model domain averaged surface heat flux is -1 W/m^2, which corresponds to a net heat loss over the basin. The corresponding value computed from the SOC air–sea climatology is a net heat gain by the ocean of 6 W/m^2. For comparison, it is well known that hydrographic measurements of the transport through the Strait of Gibraltar reveal a net heat loss over the Mediterranean Sea. In particular, Macdonald et al. (1994) find that the basin mean net heat loss is in the range -3 to -7 Wm^{-2}. The model fluxes are thus in partial agreement with the observations, in the sense that they both give a net cooling, while the SOC fluxes are biased high by about 10 W/m^2. The surface heat loss in the simulation is clearly too small, especially in winter (Fig 10A), and we attribute this to the lack of forcing by synoptic storms events. The cause of the bias in the SOC fluxes is unclear. It is likely that it is due to underestimates of the latent and sensible heat loss components of the net heat exchange as the shortwave and longwave terms have already been corrected as noted above. Several factors may give rise to underestimates in these terms including uncertainty over the transfer coefficients used to estimate the fluxes and biases in the ship observations of wind speed and atmospheric humidity (Josey et al., 1999).

The annual mean model domain averaged freshwater flux is equivalent to a net sink of ~ 0.34 m/year, which includes the effects of river sources (R) as well as evaporation and precipitation. For comparison,

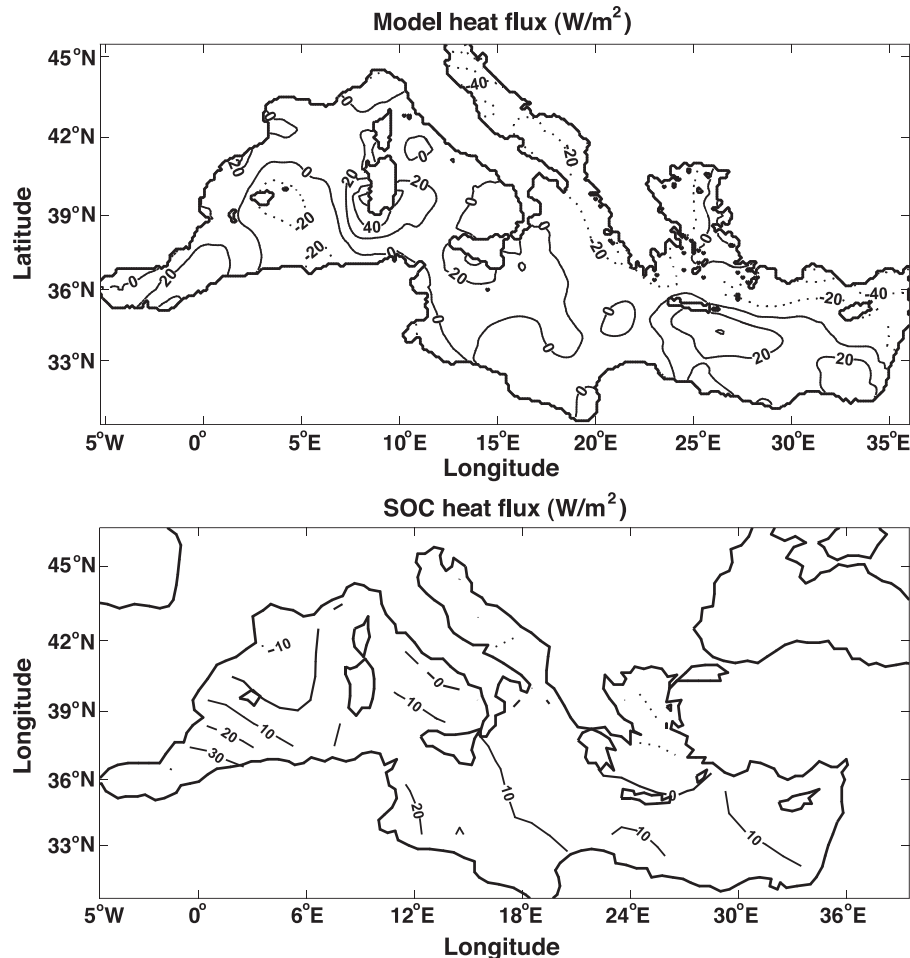**Model heat flux (W/m^2)**

SOC heat flux (W/m^2)

Fig. 11. Horizontal distribution of the model ensemble average heat flux (W/m^2) and the corresponding SOC flux climatology.

Gilman and Garret (1994) have obtained estimates of the net freshwater flux ($E - P - R$) for the basin of 0.52 m/year from the terrestrial branch of the hydrological cycle and 0.45 m/year from the aerological branch. The corresponding value for $E - P - R$ calculated from the SOC climatology is 0.53 m/year; note the SOC value has been determined using the same value for the runoff, 0.21 m/year, employed by Gilman and Garret (1994). Our model total is less than the smallest of these estimates, but we have not accounted for episodic synoptic events and the model-consistent evaporation rate is affected by any model misrepresentation of the vertical mixing of salinity. The present modified Pacanowski and Philander

(1981) approach may give too little salinity mixing (e.g., under-representation of salt fingers).

The horizontal distribution of the yearly average surface heat flux (Q) and freshwater volume source (W^{top}) needed to keep the model on track with the climatological surface data are shown in the maps of Figs. 11 and 12. For comparison with observations, we show in the same figures the corresponding observed annual averaged fluxes from the SOC climatology. As the observed fluxes are accessible at a coarse resolution of $1° \times 1°$, a running mean spatial filter has been applied to the model field to facilitate the comparison. Even so, this comparison is difficult because the observed data only captures large-scale
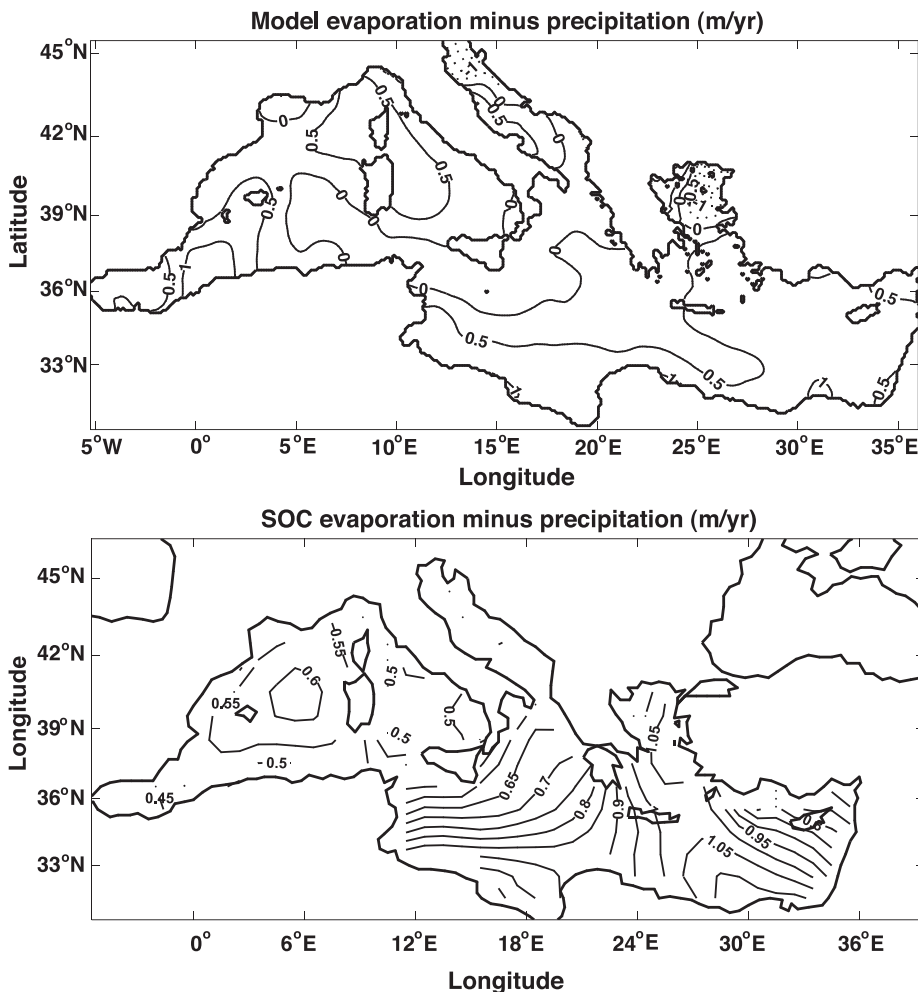

Fig. 12. Same as Fig. 11 but for the volume freshwater source (W^{top} in m/year).

features and the model-determined fluxes are very patchy. From the heat flux comparison, we capture the net heat loss in the Adriatic Sea and in the Northern Levantine basin, but not in the Gulf of Lions. The model has tight gradients of heat fluxes near the south coast of Corsica and Sicily that are not reflected in the observations. The heating of the Alboran Sea is reflected in both the model fluxes and in the observations. As regards the surface freshwater flux, we see in the model the freshening by rivers in the Adriatic and the northern Aegean, and rather strong spatial variations generally. In comparison, the SOC estimate of $E - P$ over much of the Eastern Mediterranean shows less pronounced variations (note smaller contour interval) and is stronger than the model derived value. The weaker model $E - P$ is consistent with the model salinity in this region being slightly less than the observations (Fig. 4).

5. Discussion

Wind stresses used to force ocean models are readily estimated by bulk formula based on atmospheric wind observations and meteorological model outputs. However, Q and, especially, $E - P$, are not easily measured or determined by atmospheric models, and may thus be much less accurate. Therefore, the different surface flux parameterizations or the different air–sea fluxes estimations that are available to force ocean models are less than optimal (Killworth et al., 2000).

We have presented in this paper a new surface boundary condition for an ocean model that avoids either the use of (often inaccurate) observed surface fluxes or the non-physical based technique of restoring toward observations. The nudging (restoring) is included only as a true physical process (weak damping of SST fluctuations to the atmosphere) and there is no nudging of SSS. This approach does not damp surface fronts, while producing the precise ensemble (climatological) annual cycle of surface temperature and salinity. The non-damping attribute of this technique is important because it may not quench the surface expression of the internal variability, as the fast restoring does. At the same time, the resulting model-derived fluxes will also be accurate if the ocean model internal physics is accurate. This was shown in

the ideal case in which all advection and mixing is zero (Eq. (7)).

Our diagnostic flux computation method is designed for use with ocean models forced by the atmosphere. In this new methodology we have chosen, in addition to the surface wind stress, the monthly climatological value of surface temperature and salinity (T^c and S^c) to be the model's external forcing parameters. Therefore, a model forced with this methodology cannot be used to predict changes in the ensemble mean SST and SSS which are constrained to be equal to the prescribed (T^c, S^c). Such climate scale trends in the ensemble mean of SST and SSS are more appropriately addressed by studies with ocean models that are coupled to the atmosphere; a topic quite different from the present one. Nevertheless, the present approach is well suited to the study of synoptic scale interannual fluctuations in SST and SSS (e.g., Fig. 6) precisely because the method constraints only the ensemble mean but not the instantaneous values of SST and SSS. In this respect, a study of the natural interannual variability of the Mediterranean Sea under this boundary conditions will be included in a future work.

We recognize that one of the main sources of discrepancy between model fluxes and observations in the present study comes from the absence of strong synoptic forcing events that are quite common in the Mediterranean Sea (e.g., strong gust of Mistral in the Gulf of Lyons). These events are important, for example, because they allow deep water formation to occur and therefore should be included to correctly represent the thermohaline circulation in a numerical model (Castellari et al., 2000). The model integrated surface buoyancy loss in the Gulf of Lyons is of 0.33 m²/s², which is small compared to observed values of 0.74 m²/s² in Mertens and Schott (1998). This deficiency of the present study is not a limitation of the method itself, but is due to the fact that we are using climatological values of surface temperature, salinity and winds as model external parameters. We have computed that an additional surface buoyancy loss of 0.31 m²/s² in the Gulf of Lyons region will initiate deep-water formation down to 1000 m in the model. One possible way to include synoptic event type forcing in the present configuration would be to add a stochastic variability to the winds and T^c, S^c. Another possibility would be to use more accurate

forcing, if available, and to use this proposed method to prevent model drift (see below).

In the present simulation the diagnosed fluxes, Q and W^{top}, represent the total heat and freshwater flux that forces the model (the T^{nudge} term is negligible in an ensemble average). We want to point out that the method of diagnosing the surface fluxes is easily generalized and applicable to a model simulation in which more accurate forcing, including that of synoptic scale events, is available from operational atmosphere models. In this case one simply adds the prescribed fluxes on the right hand side of Eqs. (1) and (8), respectively, and the resulting diagnosed Q and W^{top} fields become monthly mean *corrections* to the prescribed fluxes that are required to keep the model SST and SSS on track with climatology. If the ocean model's internal dynamics and forcing is sufficiently accurate, our model-inferred heat and freshwater flux will give an appropriate increment (correction) to the prescribed fluxes to reproduce the observed annual cycle ocean surface temperature and salinity. If the prescribed fluxes are accurate, the diagnosed Q and W^{top} (now seen as flux corrections) will vanish. Seen in this more general context, one can interpret the diagnosed fluxes as simply "optimal" corrections to model errors. Such model errors include inaccuracies in the prescribed forcing (wind stress and heat/freshwater fluxes) as well as internal model physics. We thus see the present method of diagnosing the surface fluxes as being useful for identifying model weaknesses. The advantage of this method (for correcting prescribed flux fields) is that it avoids the damping and/or phase errors of simple restoring methods. As a final comment, a further extension of the method could be to identify errors and to improve the parameterization of subgrid scale fluxes between model layers, again with no damping or phase lag effects.

Acknowledgements

Appendix A. Convergence of $Q(m,n)$

Here we demonstrate the convergence of $Q_{m,n}$ over a long-term model simulation and interpret the result. In practice, the convergence is complete in less than about 10 years. Let $a_{m,n}$, $n=1\ldots$ denote the heat flux adjustments shown in Eq. (5). That is,

$$a_{m,n} = [T^{\text{c}}_{m+1} - T + \sum T^{\text{nudge}}]/N,$$

as computed at the end of month m during year n. Using Eqs. (4) and (6), we have for subsequent years,

$$Q_{m,2} = Q_{m,0} + a_{m,1}/2$$

$$Q_{m,3} = Q_{m,0} + a_{m,1}/2 + a_{m,2}/3$$

$$Q_{m,4} = Q_{m,0} + a_{m,1}/2 + a_{m,2}/3 + a_{m,3}/4, \qquad \text{(A-1)}$$

and so forth. Thus,

$$Q_{m,n} = Q_{m,0} + \sum_{j=1}^{n-1} a_{m,n}/(j+1). \qquad \text{(A-2)}$$

Since the $a_{m,n}$ are bounded, it is clear that $Q_{m,n}$ converges as n increases. To examine the limit of $Q_{m,n}$ for large n, we consider the adjustments $a_{m,n}$, beginning with the first year, $n=1$. During the first year, the model is driven by $Q_{m,0}$ while at the same time (after each month) $a_{m,1}$ is computed from Eq. (5). By its construction, $a_{m,1}$ represents mostly the advection/mixing effects. This is because in the absence of such effects $Q_{m,0}$ alone will drive the model SST to T^{c}_m. On the other hand, if the $a_{m,n}$ are persistently positive, it means that T is persistently less than T^{c} (see Eq. (5)), which implies persistent cold advection and/or mixing effects at the point in question. Thus we denote

$$a_{m,1} = A_m + a'_{m,1}, \qquad \text{(A-3)}$$

where A_m represents the model climatological advection/mixing, and $a'_{m,1}$ represents that part of $a_{m,1}$ which is due to other processes such as transient fronts, anomalies in advection or mixing and so forth. From Eq. (A-1) therefore, we see that the heat flux used in the second year is

$$Q_{m,2} = Q_{m,0} + \frac{1}{2}A_m + \frac{1}{2}a'_{m,1}. \qquad \text{(A-4)}$$

Now because of the 1/2 factor multiplying A_m, which comes about because we have taken $a_{m,0} = 0$, $Q_{m,2}$ will only be sufficient to reduce the temperature difference $T_m^c - T$ by half of what its difference was in year 1. As a result, we find that in year 2

$$a_{m,2} = \frac{1}{2}A_m + a'_{m,2}.$$

Substituting Eqs. (A-3) and (A-4) into Eq. (A-1) we obtain the heat flux for year 3 as

$$Q_{m,3} = Q_{m,0} + \frac{2}{3}A_m + \frac{a'_{m,1}}{2} + \frac{a'_{m,2}}{3}. \qquad (A\text{-}5)$$

Since $Q_{m,3}$ now contains only 2/3 A_m, it will still not be able to close the gap between T_{m+1} and T in year 3. Thus, we will find that the heat flux for year 4 will be:

$$Q_{m,4} = Q_{m,0} + \frac{3}{4}A_m + \frac{a'_{m,1}}{2} + \frac{a'_{m,2}}{3} + \frac{a'_{m,3}}{4},$$

and in general,

$$Q_{m,n+1} = Q_{m,0} + \frac{n}{n+1}A_m + \sum_{j=1}^{n}\frac{a'_{m,j}}{j+1}. \qquad (A\text{-}6)$$

In those rare ocean regions where there is little or no advection and/or mixing effects at any time, $A = a' = 0$. In this situation (Eq. (A-6)) shows that $Q = Q_{m,0}$ which is the condition for a local heat balance Eq. (3). Regions with climatologically persistent cold advection, i.e., $A_m > 0$, have $Q > Q_{m,0}$ as expected. Transient advective effects represented by a' alternate in sign from month to month and therefore have a negligible influence on Q.

References

Artale, V., Iudicone, D., Santoleri, R., Rupolo, V., Marullo, S., D'Ortenzio, F., 2002. Role of surface fluxes in ocean general circulation models using satellite sea surface temperature: validation of and sensitivity to the forcing frequency of the Mediterranean thermohaline circulation. J. Geophys. Res. 107 (C8) (10.1029/2000JC000452).

Baschcek, B., Send, U., Lafuente, J.G., Candela, J., 2001. Transport estimates in the Strait of Gibraltar with a tidal inverse model. J. Geophys. Res. 106, 31017–31032.

Beckers, J.M., MEDMEX, 2002. Model intercomparison in the Mediterranean: MEDMEX simulations of the seasonal cycle. J. Mar. Syst. 33–34, 215–251.

Bignami, F., Marullo, S., Santoleri, R., Schiano, M.E., 1995. Long-wave radiation budget in the Mediterranean Sea. J. Geophys. Res. 100 (C2), 2501–2514.

Brasseur, P., Brankart, J., Schoenauen, R., Beckers, J.M., 1996. Seasonal temperature and salinity fields in the Mediterranean Sea: climatological analyses of an historical data set. Deep-Sea Res. 43, 159–192.

Bryan, K., 1969. A numerical method for the study of the circulation of the World Ocean. J. Comput. Phys. 4, 347–376.

Castellari, S., Pinardi, N., Leaman, K., 1998. A model study of air–sea interactions in the Mediterranean Sea. J. Mar. Syst. 18, 89–114.

Castellari, S., Pinardi, N., Leaman, K., 2000. Simulation of water mass formation processes in the Mediterranean Sea: influence of the time frequency of the atmospheric forcing. J. Geophys. Res. 105, 24157–24181.

Dietrich, D.E., 1997. Application of a modified 'a' grid ocean model having reduced numerical dispersion to the Gulf of Mexico circulation. Dyn. Atmos. Ocean. 27, 201–217.

Dietrich, D.E., Ko, D.-S., 1994. A semi-collocated ocean model based on the SOMS approach. Int. J. Numer. Methods Fluids 19, 1103–1113.

Fernández, V., Dietrich, D.E., Haney, R.L., Tintoré, J., 2003. Mesoscale, seasonal and interannual variability in the Mediterranean Sea using a numerical ocean model. Prog. Oceanogr. (in press).

Gilman, C., Garret, C., 1994. Heat flux parameterization for the Mediterranean Sea: the role of atmospheric aerosols and constrains from the water budget. J. Geophys. Res. 99, 5119–5134.

Haney, R.L., 1971. Surface thermal boundary condition for ocean circulation models. J. Phys. Oceanogr. 1, 241–248.

Huang, R.X., 1993. Real freshwater flux as a natural boundary condition for the salinity balance and thermohaline circulation forced by evaporation and precipitation. J. Phys. Oceanogr. 33, 2428–2446.

Hughes, C.W., 2000. A theoretical reason to expect inviscid western boundary currents in realistic oceans. Ocean Model. 2, 73–83.

Josey, S.A., Kent, E.C., Taylor, P.K., 1999. New insights into the ocean heat budget closure problem from analysis of the SOC air–sea flux climatology. J. Climate 12, 2856–2880.

Killworth, P.D., Smeed, D.A., Nurser, A.J.G., 2000. The effects on ocean models of relaxation toward observations at the surface. J. Phys. Oceanogr. 30, 160–174.

Macdonald, A., Candela, J., Bryden, H.L., 1994. An estimate of the net heat transport through the Strait of Gibraltar. In: La Violette, P.E. (Ed.), Coastal Estuarine Studies, vol. 46. AGU, Washington, DC, pp. 13–32.

Mertens, C., Schott, F., 1998. Interannual variability in deep-water formation in the northwestern Mediterranean. J. Phys. Oceanogr. 28, 1410–1424.

Myers, P., Haines, K., 2000. Seasonal and interannual variability in a model of the Mediterranean under derived flux forcing. J. Phys. Oceanogr. 30, 1069–1082.

Pacanowski, R.C., Philander, S.G.H., 1981. Parameterization of vertical mixing in numerical models of tropical oceans. J. Phys. Oceanogr. 11, 1443–1451.

Pierce, D.W., 1996. Reducing phase and amplitude errors in restoring boundary conditions. J. Phys. Oceanogr. 26, 787–805.

Rahmstorf, S., Willebrand, J., 1995. The role of temperature feed-back in stabilizing the thermohaline circulation. J. Phys. Oceanogr. 25, 787–805.

Roullet, G., Madec, G., 2000. Salt conservation, free surface, and varying levels: a new formulation for ocean general circulation models. J. Geophys. Res. 105, 23927–23942.

Roussenov, V., Stanev, E., Artale, V., Pinardi, N., 1995. A seasonal model of the Mediterranean Sea general circulation. J. Geophys. Res. 100, 13515–13538.

Sanderson, B.G., Brassington, G., 1998. Accuracy in the context of a control-volume model. Atmos. Ocean. 36, 355–384.

Seager, R., Kushnir, Y., Cane, M.A., 1995. A note on heat flux boundary conditions for ocean models. J. Phys. Oceanogr. 25, 3219–3230.

Staneva, J.V., Dietrich, D.E., Stanev, E., Bowman, M.J., 2001. Rim current and coastal eddy mechanisms in an eddy-resolving Black Sea general circulation model. J. Mar. Syst. 31, 137–157.

Viudez, A., 1997. An explanation for the curvature of the Atlantic jet past the Strait of Gibraltar. J. Phys. Oceanogr. 27, 1804–1810.

Wu, P., Haines, K., 1998. The general circulation of the Mediterranean Sea from a 100-year simulation. J. Geophys. Res. 103, 1121–1135.